22. S. R. Kim, K. Y. Lee, J. Y. Lee, *J. Alloys Compd.*, **223**, 22 (1995).
23. H. Buchner, M. A. Gutjahr, K. D. Beccu, and H. Saufferer, *Z. Metallkde.*, **63**, 497 (1972).
24. J. J. Reilly and R. H. Wiswall, *J. Inorg. Chem.*, **13**, 218 (1974).
25. G. Milazzo and S. Caroli, *Tables of Standard Electrode Potentials*, John Wiley & Sons, Inc., New York (1978).
26. *Standard Potentials in Aqueous Solution*, A. J. Bard, R. Parsons, and J. Jordan, Editors, Marcel Dekker, Inc., New York (1985).
27. J. E. A. M. van den Meerakker and J. W. G. de Bakker, *J. Appl. Electrochem.*, **20**, 85 (1990).

Effect of Methanol Crossover in a Liquid-Feed Polymer-Electrolyte Direct Methanol Fuel Cell

M. K. Ravikumar and A. K. Shukla

Indian Institute of Science, Solid State and Structural Chemistry Unit, Bangalore 560012, India

ABSTRACT

The performance of a liquid-feed direct methanol fuel cell employing a proton-exchange membrane electrolyte with Pt-Ru/C as anode and Pt/C as cathode is reported. The fuel cell can deliver a power density of *ca.* 0.2 W/cm^2 at 95°C, sufficient to suggest that the stack construction is well worthwhile. Methanol crossover across the polymer electrolyte at concentrations beyond 2 *M* methanol affects the performance of the cell which appreciates with increasing operating temperature.

Introduction

Electric vehicles powered with polymer-electrolyte fuel cells using hydrogen as fuel are presently being tested for vehicular applications.[1] But hydrogen is difficult both to store and transport. The most satisfactory approach seems to be to electro-oxidize a liquid fuel at the anode. Methanol is the only liquid fuel that has any substantial electroactivity and can be directly oxidized to carbon dioxide and water on catalytically active anodes in a direct methanol fuel cell (DMFC).[2,3] However, the fundamental limitation in the practical utilization of such fuel cells has been the existence of electrochemical losses at both the anode and cathode, leading to poor overall conversion efficiencies.[4,5]

Recently, a liquid-feed polymer-electrolyte DMFC with power outputs near 0.15 W/cm^2 at operational temperatures close to 90°C has been reported by Surampudi *et al.*[6] In this communication, we report a liquid-feed polymer-electrolyte DMFC with power densities of *ca.* 0.2 W/cm^2 at an operational temperature of 95°C which is achieved by combining the improved catalysts with fuel cell engineering. These developments are encouraging for stack construction. Since Nafion (the most commonly employed polymer-electrolyte membrane) has the drawback of permeability to methanol leading to a mixed potential at the cathode which reduces the overall cell potential, we have also conducted a study on distinct *in situ* determination of anode and cathode performance in the DMFC at various methanol concentrations and operating temperatures. It is found that methanol crossover across the polymer-electrolyte membrane in such a liquid-feed DMFC affects its performance beyond 2 *M* concentration, particularly at higher temperatures. These data are seminal for practical realization of DMFCs.

Experimental

Preparation of $Na_6Pt(SO_3)_4$ and $Na_6Ru(SO_3)_4$ precursors.— $Na_6Pt(SO_3)_4$ and $Na_6Ru(SO_3)_4$ were used as precursors for catalyst preparation. $Na_6Pt(SO_3)_4$ was prepared by dissolving 1 g H_2PtCl_6 in 100 ml distilled water and the pH of the solution adjusted to 7 by adding Na_2CO_3. Solution pH was subsequently lowered to 3 by adding $NaHSO_3$. The solution was then gently warmed until it became colorless. Solution pH was raised to 6 by adding Na_2CO_3 when a white precipitate of $Na_6Pt(SO_3)_4$ was obtained, which was filtered, washed copiously with distilled water to remove chloride ions, and dried in an air oven at 80°C for 2 h.[7-9]

$Na_6Ru(SO_3)_4$ was prepared by dissolving 207 mg anhydrous $RuCl_3$ in 50 ml of 0.1 *N* HCl. The pH of the solution was adjusted to 7 by adding Na_2CO_3. Then solution pH was lowered to 3 by adding $NaHSO_3$. After heating the solution at 80°C for 30 min, solution pH was raised to 6 by adding Na_2CO_3, when a grayish blue precipitate of $Na_6Ru(SO_3)_4$ was obtained which was filtered, washed copiously with distilled water, and dried in an air oven at 80°C for 2 h. Formation of these precursors was confirmed by their infrared spectra.

Preparation of Pt/C.—The required amount of Ketjen-Black (EC) 600-TD (Akzo Chemie) carbon (80 mg) was suspended in distilled water and agitated in an ultrasonic water bath at 80°C to form carbon slurry. 400 mg of $Na_6Pt(SO_3)_4$ was dissolved in 50 ml 1 *N* H_2SO_4 and diluted to 150 ml with distilled water and was added drop by drop to the carbon slurry with constant stirring at 80°C. 50 ml of H_2O_2 (30%) was slowly added to this solution with temperature maintained at 80°C, which results in vigorous gas evolution upon stirring for 1 h. The platinized-carbon substrate was obtained by reducing with 1 weight percent (w/o) formic acid solution, which was washed copiously with hot distilled water, filtered, and dried in an air oven at 80°C for 2 h.

The variation in potential during the preparation of the Pt/C is recorded *in situ* using a spiral platinum electrode *vs.* a mercury-mercurous sulfate (MMS) reference electrode. The concomitant change in pH during the preparation was also recorded employing a temperature-compensated pH probe.

Preparation of Pt-Ru/C.—The required amount of KetjenBlack carbon (33 mg) was suspended in water (50 ml) and agitated in an ultrasonic agitator to form a thick carbon slurry. 653 mg of $Na_6Pt(SO_3)_4$ was dissolved in 50 ml of 1 *N* H_2SO_4 and diluted to 750 ml with distilled water. The pH of the solution was adjusted to 5 by adding 10 w/o NaOH solution. Then 100 ml of H_2O_2 (30%) was added drop by drop with constant stirring. The pH of the solution was adjusted to 5. To this solution 560 mg $Na_6Ru(SO_3)_4$ dissolved in 150 ml of 1 *N* H_2SO_4 was added drop by drop. The pH of the solution was again adjusted to 5 after the gas evolution ceased. The carbon slurry was now slowly added under constant stirring. Hydrogen gas was bubbled through this admixture for 1 h, and the suspension was allowed to settle, filtered, washed copiously with hot distilled water, and dried in an air oven at 80°C for 2 h. The variations in potential and pH during the preparation of the catalyzed substrate were monitored.

Both the Pt/C and Pt-Ru/C substrates are characterized by their x-ray diffraction patterns obtained on a JEOL

JDX-8P x-ray diffractometer (λ = 1.5418 Å). Pt-Ru/C samples are also characterized by using energy dispersive analysis by x-rays (EDAX) on a scanning electron microscope Model S-150 Stereoscan Cambridge (UK) in order to ascertain Pt:Ru composition in the catalyst samples. Size distribution and morphology of the catalyst particles in both the Pt/C and Pt-Ru/C were examined with a JEOL JEM-200CX high-resolution electron microscope (HREM). For this purpose specimens were prepared by ultrasonically suspending the catalyst powder in acetone. A drop of the suspension was then placed on 3 mm holey carbon-coated grids and dried in air. Electron diffraction and images were recorded in different regions.

Membrane electrode assembly.—Both the anode and cathode consist of a backing layer, a gas-diffusion layer, and a reaction layer. A Teflonized carbon paper (Kureha) of 0.3 mm thickness is employed as the backing layer in these electrodes. To prepare the gas-diffusion layer, KetjenBlack carbon was suspended in water and agitated in an ultrasonic bath. To this 10 w/o Teflon (Fluon-GP2) suspension was added with continuous agitation and the required amount of cyclohexane added drop by drop. The resultant slurry was spread onto the Teflonized carbon paper and dried in an air oven at 80°C for 2 h. To prepare the reaction layer, the required amount of Pt/C (cathode) or Pt-Ru/C (anode) was mixed with 10 w/o Teflonized carbon obtained by mixing activated carbon with 10 w/o Teflon suspension, followed by heating in an air oven at 350°C for 30 min. This mixture was suspended in water and agitated in an ultrasonic water bath, and a 15 w/o Nafion solution (Aldrich) was added to it with continuous stirring. The paste thus obtained is spread onto the gas-diffusion layer of the electrode and pressed at 75 kg/cm^2 for 5 min. The Pt content in both the cathode and anode was maintained at about 5 mg/cm^2. A thin layer of Nafion solution was spread on the surface of each electrode. The membrane electrode assembly (MEA) was obtained by pressing the cathode and anode on either side of a pretreated Nafion-117 proton exchange membrane by compaction with a pressure of 50 kg/cm^2 at 125°C for 3 min. The MEA is about a millimeter in thickness.

Fuel cell assembly.—A liquid-feed polymer-electrolyte DMFC was assembled employing the membrane electrode assembly. The anode and cathode were contacted on their rear with gas/fluid-flow field plates machined from high-density graphite blocks in which channels were formed. The channels were machined to achieve minimum mass-polarization in the DMFC. The ridges between the channels make electrical contact with the backs of the electrodes and conduct the current to the external circuit. The channels supply the fuel (methanol) to the anode and oxidant (oxygen) to the cathode. Electrical heaters were placed behind each of the graphite blocks in order to heat the cell to the desired operational temperature. The methanol solution was pumped to the anode chamber through a peristaltic pump and the unreacted methanol solution is collected back in the reservoir. Oxygen gas at about 4 bar pressure was introduced into the cathode chamber. The graphite blocks were also provided with connectors for electrical contacts and tiny holes to accommodate thermocouples. A dynamic hydrogen electrode (DHE) was prepared by coupling two palladium-gold grids (5 × 5 mm) onto the Nafion membrane, as shown in Fig. 1. A small dc voltage was imposed between these electrodes. The negative electrode that generates hydrogen was used as the reference electrode. This reference electrode was calibrated against a bubbling hydrogen electrode, and the current through the DHE was adjusted to give a potential difference of ~1 mV. The experimental fuel cell along with the DHE is shown schematically in Fig. 1. Galvanostatic polarization data on the activated DMFC were obtained at various methanol concentrations and temperatures. The experiments were conducted on several MEAs to ascertain the reproducibility of the data. The active geometrical area of the electrodes was 4 cm^2. The current densities were calculated based on the active geometrical area of the electrodes.

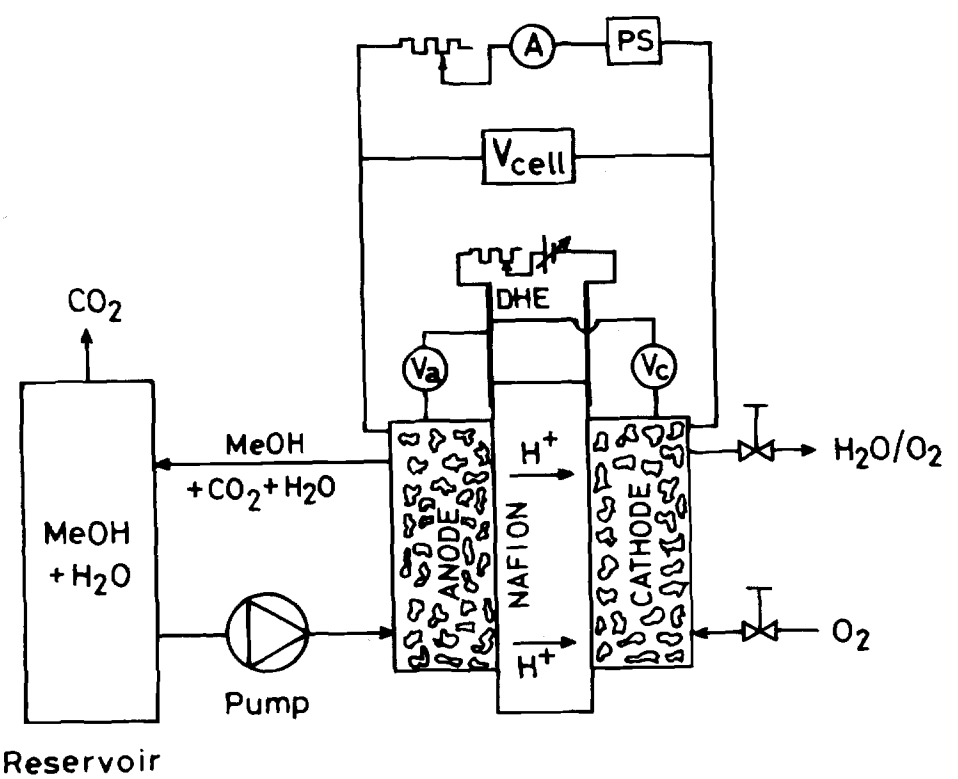

Fig. 1. Schematic representation of the liquid-feed polymer-electrolyte DMFC (DHE-dynamic hydrogen electrode, V_{cell}-cell voltage, V_a-anode potential *vs.* DHE, V_c-cathode potential *vs.* DHE, A-ammeter, and PS-dc power supply).

Results

Characterization of Pt/C and Pt-Ru/C.—Variations in potential and pH during the preparation of the Pt/C are shown in Fig. 2a-c. During the impregnation of carbon with $Na_6Pt(SO_3)_4$ solution, the potential first increases in the anodic direction and attains a constant value at about 170 mV *vs.* MMS, corresponding to the Pt^{2+}/Pt° redox couple (Fig. 2a).[10] On addition of H_2O_2 to this admixture, initially the potential shifts cathodically by 20 mV and remains invariant thereafter (Fig. 2b). The potential shifts cathodically with an inflexion point at 100 mV *vs.* MMS during reduction by HCOOH (Fig. 2c), and most of the reduction is complete with 10 ml of 1 w/o of HCOOH. The pH of the medium remains acidic during the preparation of Pt/C.

The variations in potential and pH during the preparation of Pt-Ru/C are shown in Fig. 3a-c. During the addition of H_2O_2 to $Na_6Pt(SO_3)_4$ solution, potential increases sharply in the beginning with a concomitant decrease in pH, as shown in Fig. 3a. The observed potential corresponds to the Pt^{2+}/Pt° redox couple. The decrease in pH could be attributed to the acidity of H_2O_2. During addition of $Na_6Ru(SO_3)_4$ to this solution, the potential increases anodically with decrease in pH, as shown in Fig. 3b. This may be due to the oxidation of Ru^{2+} to Ru^{4+} following the reaction[11]

$$Ru^{2+} + H_2O_2 \rightarrow RuO_2 + 2H^+$$

The excess H_2O_2 decomposes to yield water and oxygen. As shown in Fig. 3c, the potential increases cathodically during the reduction by hydrogen gas, which seems to be complete within about 30 min.

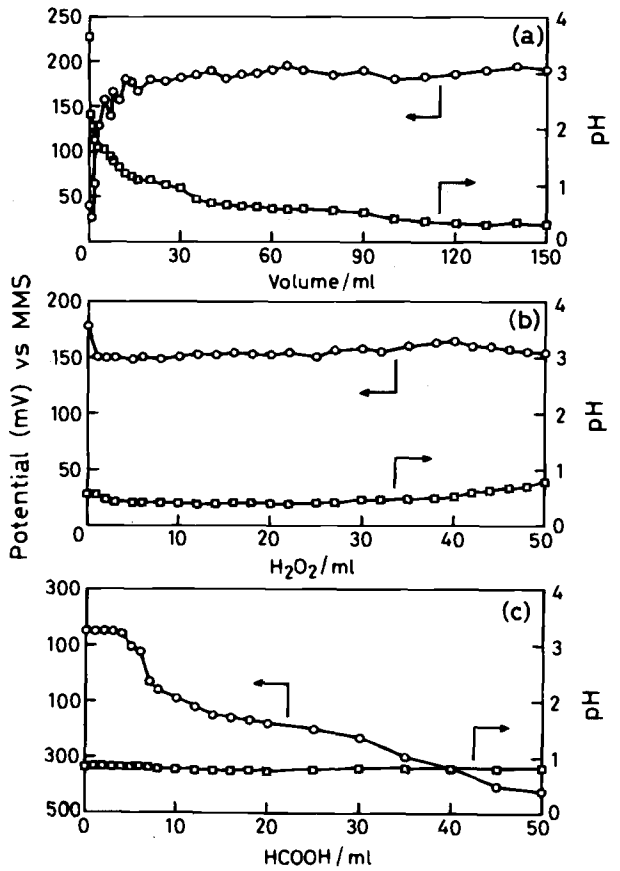

Fig. 2. Variations in potential and pH during the preparation of Pt/C: (a) impregnation of carbon with $Na_6Pt(SO_3)_4$ solution, (b) addition of H_2O_2, and (c) reduction with HCOOH.

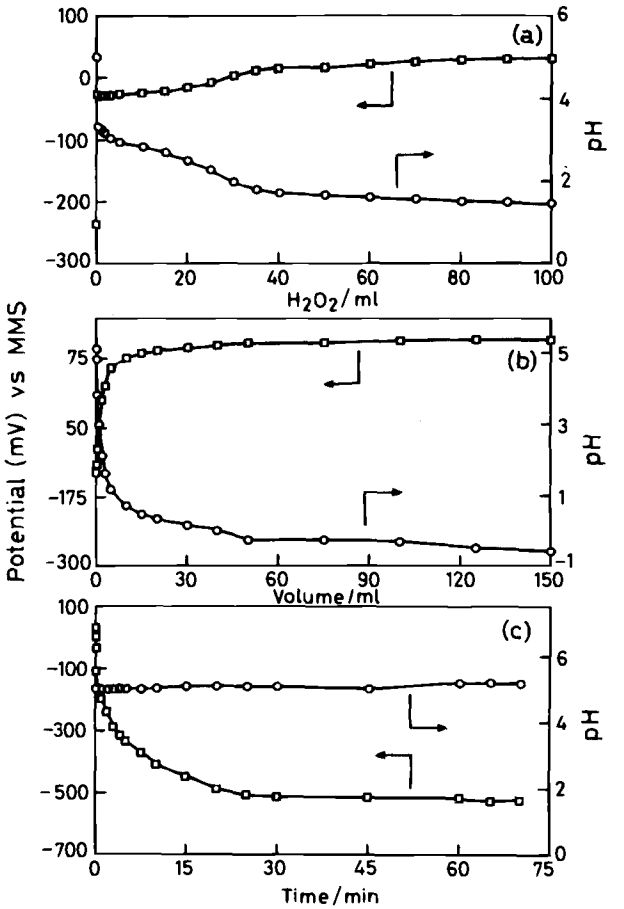

Fig. 3. Variations in potential and pH during preparation of Pt-Ru/C: (a) addition of H_2O_2 to $Na_6Pt(SO_3)_4$ solution, (b) addition of $Na_6Ru(SO_3)_4$ solution, and (c) reduction with H_2 gas.

The x-ray diffraction patterns of Pt/C and Pt-Ru/C samples are shown in Fig. 4a and b, respectively. It is found that the average particle size of Pt crystallites in Pt/C is about 30 Å while Pt-Ru/C is x-ray amorphous. The latter on heat-treatment in vacuum (10^{-5} Torr) at 500°C for 3 h is found to be crystalline (Fig. 4c) and shows presence of a

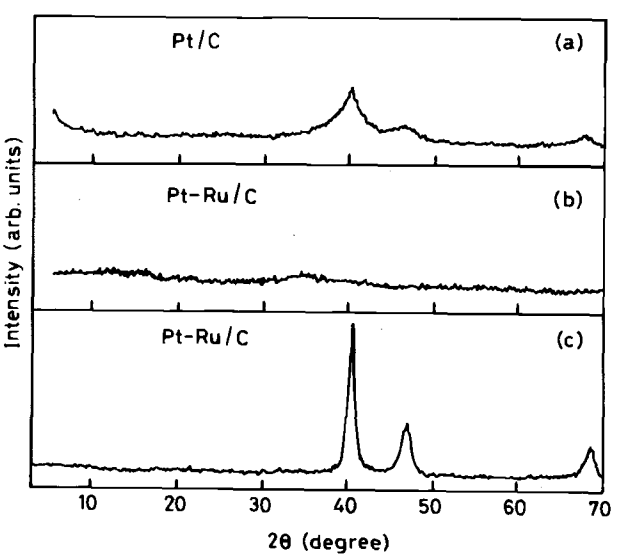

Fig. 4. X-ray powder diffraction patterns for the samples (a) Pt/C, (b) Pt-Ru/C, and (c) Pt-Ru/C after heat-treatment in vacuum (10^{-5} Torr) at 500°C for 3 h.

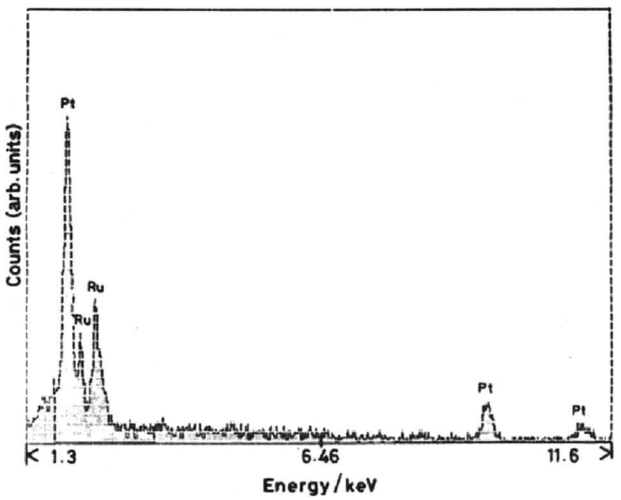

Fig. 5. EDAX spectrum of the Pt-Ru/C catalyst.

cubic phase similar to Pt, with peak positions shifted toward higher angles, suggesting a decrease in cell parameters typically associated with the formation of a Pt-Ru alloy.[12-13] The EDAX analysis of the sample given in Fig. 5 suggested the nominal composition of the catalyst to be 56Pt-44Ru.

The electron micrograph of Pt/C shown in Fig. 6a suggests that the Pt particles are about 27 Å in size and are uniformly distributed. The electron diffractogram of this sample, shown in Fig. 6b, indicates a typical face-centered cubic (fcc) pattern of a Pt crystallite. By contrast, the Pt-Ru/C specimen contains amorphous Pt-Ru crystallites (Fig. 6d); the average particle size of the crystallites is 10 Å, as shown in Fig. 6c. Radmilovič *et al.*[14] have determined the chemical composition and other structural features of their supported Pt-Ru catalyst employing an analytical microscope. We, however, could not determine the chemical composition of Pt and Ru in our Pt-Ru/C specimen by HREM due to lack of an analytical facility.

Fuel cell performance.—After allowing 24 h to condition a new MEA in the test fuel cell at 60°C under atmospheric oxygen pressure with continuous feed of 2 *M* methanol, the performance characteristics of the cell were obtained at various temperatures. The galvanostatic polarization data on the liquid-feed DMFC at 70°C and 4 bar oxygen pressure with varying methanol concentrations are shown in Fig. 7a-c. It is found from the cell performance data shown in Fig. 7a that the limiting current value increases with methanol concentration and an optimum power density of 0.15 W/cm^2 is obtained with 2.5 *M* methanol. The single electrode polarization data for the oxygen and methanol electrodes with varying methanol concentrations are shown in Fig. 7b and c, respectively. It is seen that the performance of the methanol electrode increases with methanol concentration and shows a polarization of 450 mV *vs.* DHE at a load current density of 400 mA/cm^2 with 2.5 *M* methanol. However, an opposite effect is

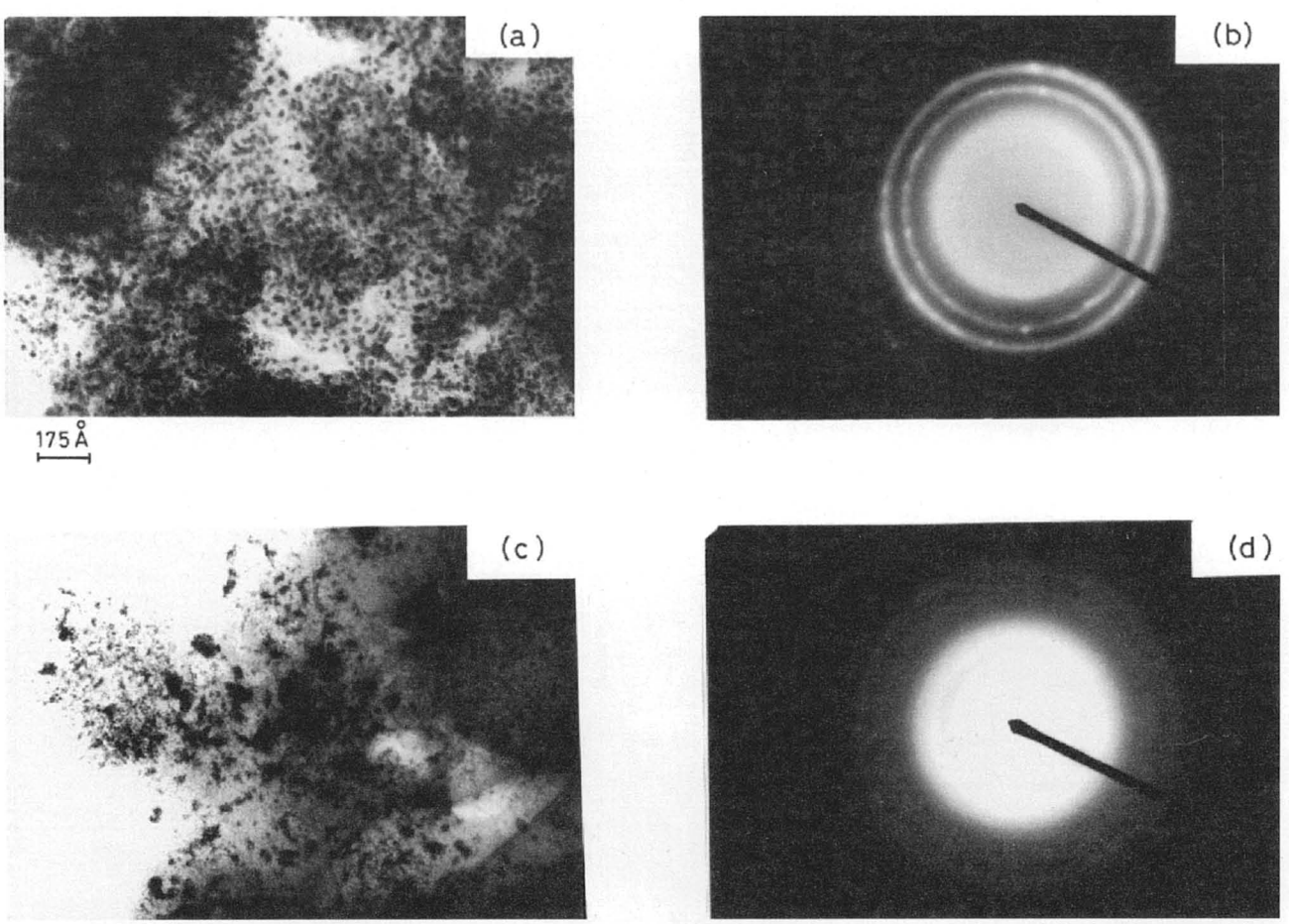

Fig. 6. (a) Electron micrograph of Pt/C. (b) Electron diffraction pattern of Pt/C. (c) Electron micrograph of Pt-Ru/C. (d) Electron diffraction pattern of Pt-Ru/C.

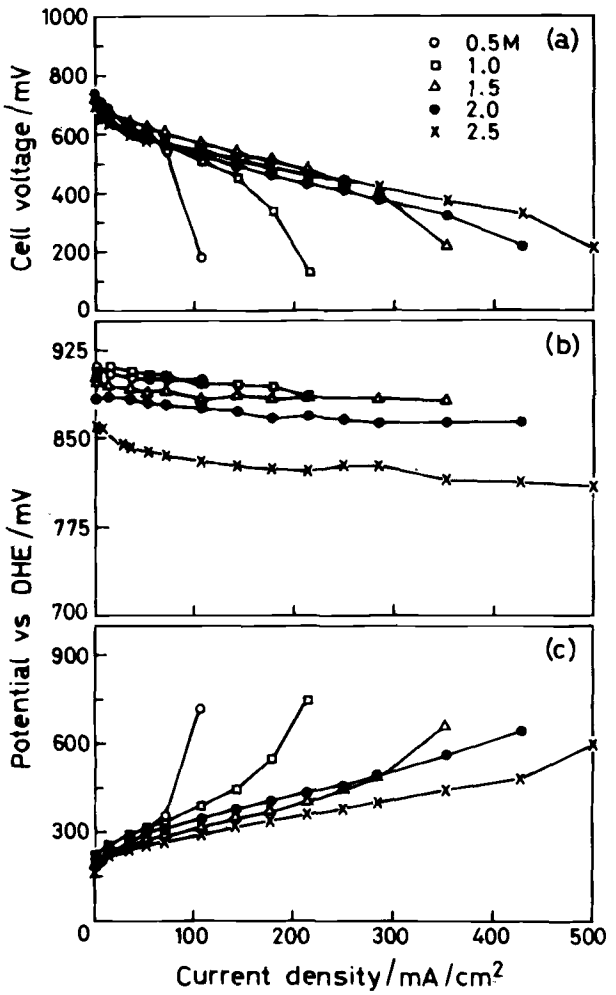

Fig. 7. Galvanostatic polarization data for (a) the liquid-feed DMFC, (b) its cathode, and (c) anode obtained at 70°C with varying methanol concentrations and 4 bar oxygen pressure.

observed for the oxygen electrode. The open-circuit potential of the oxygen electrode decreases by about 50 mV during cell operation with 2.5 *M* methanol as opposed to the value observed with 0.5 *M* methanol (Fig. 7b).

The data on performance of the liquid-feed DMFC at 95°C and 4 bar oxygen pressure with varying methanol concentrations are shown in Fig. 8a-d. The cell delivers a power density of 0.18 W/cm^2 at a load current density of 700 mA/cm^2 during operation with 2 *M* methanol (Fig. 8d). The data suggest that methanol crossover does not affect the performance of the cell up to the fuel concentration of about 2 *M* methanol. Cell performance, however, drastically decreases during cell operation with fuel concentrations beyond 2 *M* methanol (Fig. 8a). By contrast, the cell could be operated with 2.5 *M* methanol solution at 70°C, indicating that methanol crossover in the cell is higher at 95°C. This behavior is clearly reflected in the single electrode polarization data for the oxygen and methanol electrodes at 95°C shown in Fig. 8b and c, respectively. It is seen that oxygen electrode performance is drastically affected during cell operation with 2.5 *M* methanol solution, which reduces overall cell potential. The data on the endurance test of the cell conducted with 2 *M* methanol and about 4 bar oxygen pressure at 70 and 95°C are shown in Fig. 9. It is noteworthy that the more developed hydrogen-oxygen polymer-electrolyte membrane fuel cells that are nearing commercialization employ pressurized oxygen and hydrogen upto 10 bar.[15]

Conclusion

It is demonstrated that the power outputs of *ca.* 0.2 W/cm^2 are achievable with liquid-feed DMFCs. *In situ* study of anode and cathode polarization in the liquid-feed DMFC suggests that cell performance is mainly limited by polarization loss at the cathode due to methanol crossover, which increases both with temperature and methanol concentration. The membrane treatments which would lower the flux of methanol at the cathode will help to improve cell performance.

Acknowledgment

We thank Professor K.S. Gandhi, Department of Chemical Engineering, Indian Institute of Science, Bangalore, for many helpful discussions. We also thank Dr. G. N. Subbanna, Materials Research Center of this Institute, for recording electron diffraction patterns and micrographs. Financial support from the Ministry of Non-conventional Energy Sources, Government of India, New Delhi, is gratefully acknowledged.

Manuscript submitted Dec. 18, 1995; revised manuscript received April 13, 1996.

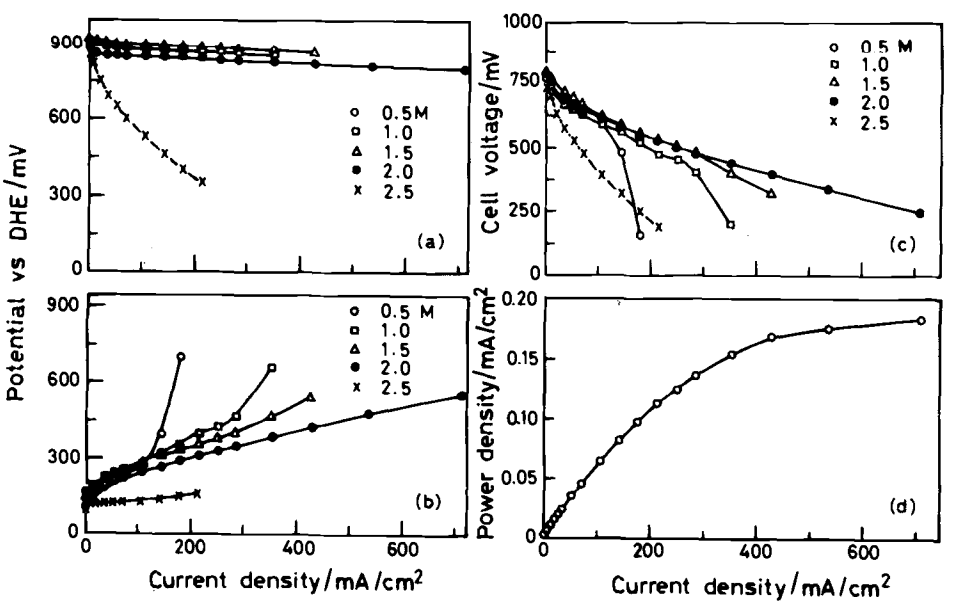

Fig. 8. Galvanostatic polarization data for the liquid-feed DMFC obtained with varying methanol concentrations and 4 bar oxygen pressure at 95°C: (a) its cathode, (b) its anode, (c) the cell performance, and (d) the optimum power output obtained from DMFC during its operation at 95°C with 2 *M* methanol and about 4 bar O_2 pressure.

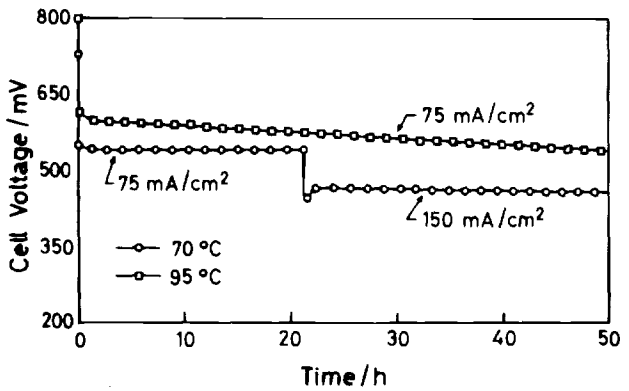

Fig. 9. Data on endurance test of the liquid-feed DMFC conducted at different temperatures with 2 *M* methanol concentration and about 4 bar oxygen pressure.

REFERENCES

1. K. B. Prater, *J. Power Sources*, **51**, 129 (1994).
2. W. Vielstich, A. Küver, M. Krausa, A. C. Ferreira, K. Petrow, and S. Srinivasan, in *Batteries and Fuel Cells for Stationary and Electric Vehicle Applications*, A. R. Langrebe and Z. Takehara, Editors, PV 93-8, p. 269, The Electrochemical Society Proceeding Series, Pennington, NJ (1993).
3. J.-M. Léger and C. Lamy, *Ber. Bunsenges. Phys. Chem.*, **94**, 1021 (1990).
4. R. Parsons and T. Vandernoot, *J. Electroanal. Chem.*, **257**, 9 (1987).
5. A. Hamnett and G. L. Troughton, *Chem. Ind.*, 480 (July 1992).
6. S. Surampudi, S. R. Narayanan, E. Vamos, H. Frank, G. Halpert, A. Laconti, J. Kosek, G. K. Surya Prakash, and G. A. Olah, *J. Power Sources*, **47**, 377 (1994).
7. H. G. Petrow and R. J. Allen, U.S. Pat. 3,992,331 (1976).
8. H. G. Petrow and R. J. Allen, U.S. Pat. 3,992,512 (1976).
9. H. G. Petrow and R. J. Allen, U.S. Pat. 4,044,193 (1975).
10. J. F. Llopis and F. Colom, in *Encyclopedia of Electrochemistry of the Elements*, A. J. Bard, Editor, Vol. 6, p. 169, Marcel Dekker, Inc., NewYork (1976).
11. M. Watanabe, M. Uchida, and S. Motoo, *J. Electroanal. Chem.*, **229**, 395 (1987).
12. H. Miura, T. Suzuki, Y. Ushikubo, K. Sugiyama, T. Matsuda, and R. D. Gonzalez, *J. Catal.*, **85**, 331 (1984).
13. H. A. Gesteiger, N. Marković, P. N. Ross, Jr., and E. J. Cairns, *J. Phys. Chem.*, **97**, 12,020 (1993).
14. V. Radmilovič, H. A. Gesteiger, and P. N. Ross, Jr., *J. Catalysis*, **154**, 98 (1995)
15. O. J. Murphy, G. D. Hitchens, and D. J. Manko, *J. Power Sources*, **47**, 353 (1994).

Chemical Diffusion Coefficient of Lithium in Carbon Fiber

Takashi Uchida, Yasuyuki Morikawa, Hiromasa Ikuta, and Masataka Wakihara*

Department of Chemical Engineering, Tokyo Institute of Technology, Ookayama, Meguro-ku, Tokyo 152, Japan

Kimihito Suzuki

Advanced Materials and Technology Research Laboratories, Nippon Steel Corporation, Nakahara-ku, Kawasaki 211, Japan

ABSTRACT

Electrochemical investigations on coal pitch-based carbon fiber (heat-treated at 2800°C) were carried out. The open-circuit voltages of the Li|Li_xC_6 cell were lower than 0.15 V *vs.* Li/Li^+ in the range of $0.15 < x < 0.65$. The open-circuit voltage profile *vs.* x showed no distinct two-phase region in the present Li-carbon system in $0 < x < 0.65$. Almost constant capacity of 220 mAh/g was observed until the 140th cycle in the cycling tests of the Li|carbon fiber cell (current density 25 mA/g). The compositional variation of the chemical diffusion coefficient of lithium $\tilde{D}_{Li}$ at ambient temperature was measured by two different methods, *i.e.*, the current pulse relaxation method and the potential step chronoamperometric method. Excellent agreement within one order of magnitude was observed between the two sets of $\tilde{D}_{Li}$ values obtained from these two methods. The values were around $10^{-9.5}$ cm^2/s at $x \fallingdotseq 0$ and decreased with increasing x. The $\tilde{D}_{Li}$ values lay between 10^{-11} and 10^{-12} cm^2/s in $x > 0.2$

Introduction

In order to obtain safer and more reversible negative electrodes for lithium secondary batteries, intensive research on various carbon materials, such as pyrolytic carbon, polyacrylonitrile- (PAN) based carbon, petroleum coke-based carbon, pitch-based carbon, etc., has been carried out in recent years.[1-7] The major interest in these works has been in charge-discharge capacities, cycling stabilities, crystal chemistry on lithium intercalation, and so on, and only very few reports have been published on the diffusion coefficient of lithium in the carbon anodes.[8] Morita *et al.*[8] have reported the diffusion coefficient of lithium in a pitch-based carbon fiber in two different nonaqueous electrolyte solutions. On the other hand, many studies on the diffusion coefficients of lithium ($\tilde{D}_{Li}$) in various cathode materials have been reported so far. In these studies, several kinds of electrochemical methods were used to estimate the $\tilde{D}_{Li}$ values, namely, the current pulse relaxation (CPR)[9] method, the galvanostatic intermittent titration technique (GITT),[10] the ac impedance method using Warburg impedance,[11] and potential step chronoamperometry (PSCA),[12,13] etc. Usually, one of these methods is used to estimate $\tilde{D}_{Li}$. However, the equations used in these methods contain varieties of factors, *e.g.*, open-circuit voltage (OCV) for a certain lithium composition, slope of the OCV *vs.* composition curve, surface area of the electrode, etc., some of which are sometimes rather difficult to determine exactly, and it sometimes happens that the $\tilde{D}_{Li}$ values for the same material reported in the literature differ by several orders of magnitude.

Accordingly, it would be necessary to evaluate these electrochemical methods themselves, first. We have attempted this, by measuring the $\tilde{D}_{Li}$ values in pitch-based

* Electrochemical Society Active Member.